Journal of Power Sources 196 (2011) 8598–8603

Contents lists available at ScienceDirect

Journal of Power Sources

journal homepage: www.elsevier.com/locate/jpowsour

Self-discharge behavior and its temperature dependence of carbon electrodes in lithium-ion batteries

Takashi Utsunomiya[a,b], Osamu Hatozaki[b], Nobuko Yoshimoto[a], Minato Egashira[a], Masayuki Morita[a,*]

[a] Department of Applied Chemistry, Graduate School of Science and Engineering, Yamaguchi University, 2-16-1, Tokiwadai, Ube 755-8611, Japan
[b] Subaru Technical Research Center, Fuji Heavy Industries Ltd., 9-6-3, Ohsawa, Mitaka 181-8577, Japan

ARTICLE INFO

Article history:
Received 19 April 2011
Received in revised form 14 May 2011
Accepted 24 May 2011
Available online 31 May 2011

Keywords:
Self-discharge
Graphite
Hard carbon
Lithium-ion battery
Temperature dependence

ABSTRACT

Self-discharging characteristics of negative electrodes with different carbon materials have been investigated by monitoring the open circuit potential (OCP), the capacity loss and the ac impedance change during the storage at different temperatures. The OCP change with the storage time reflected state-of-charge (SOC), which depended on both the carbon material and the storage temperature. Higher specific surface area of the material and higher storage temperature lead to higher self-discharging rate. The activation energy for self-discharging was estimated from the temperature dependence of the self-discharging rate. Although small difference was observed among the materials, the value of the activation energy suggests that the self-discharging reaction at each electrode is controlled by a diffusion process. Changes in the interfacial resistance with the storage time reflected the growth of so-called Solid Electrolyte Interphase (SEI) at carbon surface. The rate of SEI formation at lower temperature does not depend on the carbon material, but at higher storage temperature the rate on spherical graphite was much higher than those on the other carbon materials.

1. Introduction

Lithium-ion battery (LIB) has become the most important energy-storage device for many applications such as cellar phones, mobile computers and other electronic devices. The energy density of LIB has so far been improved mainly by optimizing the carbon negative electrode and the organic electrolyte solutions. More recently, much attention has been focused on the application of LIBs to the power-train of electric vehicle (EV) systems, where higher performance and larger sizes of the batteries are needed than those in portable electronics uses. Especially, the safety issue has become more important in large-size LIB technology for the EV uses. Batteries in vehicle will be under different operation modes from those in portable electronics. For instance, as the vehicles are used in the open air, the batteries are subjected to damages with alternating temperature not only for cell operation but also during the storage, from hot summer to cold winter. Moreover, the parking time is generally much longer than the driving time, which causes the capacity loss of the battery by self-discharging even under the full charge conditions. Thus, understanding the self-discharge behavior of each electrode, especially under different temperature conditions, has become more and more important to design and develop larger-sizes of LIBs [1,2].

With respect to graphite-based negative electrodes, for instance, Yazami and co-workers have reported the contribution of the self-discharge process to the capacity loss of the overall LIB system, and proposed self-discharge mechanisms deduced from their experimental results [3,4]. The main cause of the capacity loss of the negative electrode is considered to be certain chemical processes occurring at the electrode/electrolyte interface during the storage. Contribution of so-called Solid-Electrolyte-Interphase (SEI) formation to the self-discharging processes is discussed in detail [3]. The present authors have also investigated the self-discharge processes of carbonaceous electrodes with monitoring the variations in the open-circuit potential (OCP). Differences in the potential variations between graphite and polyacene semiconductor (PAS) electrodes are discussed [5].

In the present work, three kinds of carbon materials with different shape and micro-structure have been examined. The self-discharge behavior was monitored under different storage temperatures. That is, variations in OCP with storage time were recorded as a function of the temperature. The self-discharge rates were also estimated from the residual discharge capacity after the storage, and their temperature dependences were discussed from the viewpoint of the changes in the process at the electrode/electrolyte interface.

* Corresponding author. Tel.: +81 836 85 9211; fax: +81 836 85 9201.
E-mail address: morita@yamaguchi-u.ac.jp (M. Morita).

0378-7753/$ – see front matter © 2011 Elsevier B.V. All rights reserved.
doi:10.1016/j.jpowsour.2011.05.066

Table 1
Specific surface area, XRD and Raman characteristics of carbon samples examined.

Symbol	Code/company	Classification	Specific surface area ($m^2\ g^{-1}$)	d_{002} (nm) in XRD	G/D in Raman
HC	CPS(F)/Kureha	Hard carbon, crushed	3.1	3.870	0.558
FG	KS4/Timical	Synthetic graphite, flake	21.7	3.366	2.309
SG	AZ/Nippon Carbon	Natural graphite, spherical	3.4	3.363	0.926

2. Experimental

Three kinds of powdered carbon, hard carbon (HC) received from Kureha, artificial (synthetic) flake graphite (FG) from Timcal, and spherical natural graphite (SG) from Nippon Carbon, were used as the active material of the negative electrode. Typical Raman spectra of the powdered samples are shown in Fig. 1. The specific surface area, XRD characteristics and relative intensity (G/D ratio) in Raman spectra of the materials are listed in Table 1. The test electrode was composed of 88% (in mass) of the active material, 5% of carbon black, 3% of polymeric dispersant (carboxymethylcellulose, CMC) and 4% of binder (styrene-butadiene rubber, SBR). Slurry of the active material with the dispersant and the binder was made in distillated water, which was coated on a copper-foil current collector. The thickness of the active material was controlled to ca. 25 μm.

A laminate type three-electrode cell consisting of the carbon-based negative electrode as the test electrode was used. In the present experiment, a chip of lithium (Li) foil and a large surface area Li foil were used as reference and counter electrodes, respectively, in order to avoid possible influences caused by conventional positive electrode materials on the self-discharging behavior of the test electrodes. A geometric area of 20 mm × 20 mm was used as the working area of the test electrode. The electrolytic solution was 1.2 mol dm^{-3} (M) $LiPF_6$ dissolved in mixed solvent of ethylene carbonate (EC) and diethyl carbonate (DEC) with 1:3 volume ratio (1.2 M $LiPF_6$/EC3DEC). The water content in the electrolyte solution was less than 20 ppm.

The charge and discharge cycling was carried out under a constant-current condition coupled with constant-potential (CC–CP) charging, where the term "charging" means the cathodic lithiation of the negative electrodes and the "discharging" the anodic de-lithiation. Constant current of 1 mA, which is equivalent to C/10 rate, was applied for charging and discharging of the negative electrode. The cut-off potential and time for charging were 20 mV (for HC) or 30 mV vs. Li/Li^+ (for FG and SG) and 10 h, respectively.

The OCP and equivalent series resistance (ESR) were monitored for ca. 24 h after the first charging in a thermostatically controlled oven. The storage temperature was ranged from −20 °C to 60 °C. An ac impedance method was applied to analyze the interfacial processes during the storage of the charged electrodes. The frequency was scanned from 100 kHz to 10 mHz with 10 mV_{p-p} ac amplitude under the OCP conditions at room temperature. All electrochemical measurements were carried out under a dry argon atmosphere.

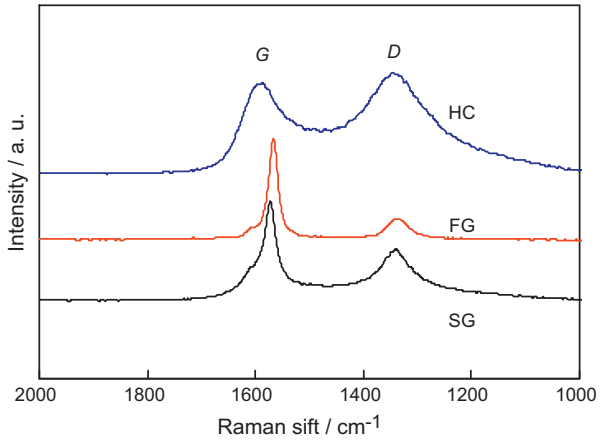

Fig. 1. Raman spectra of carbon samples examined in this work.

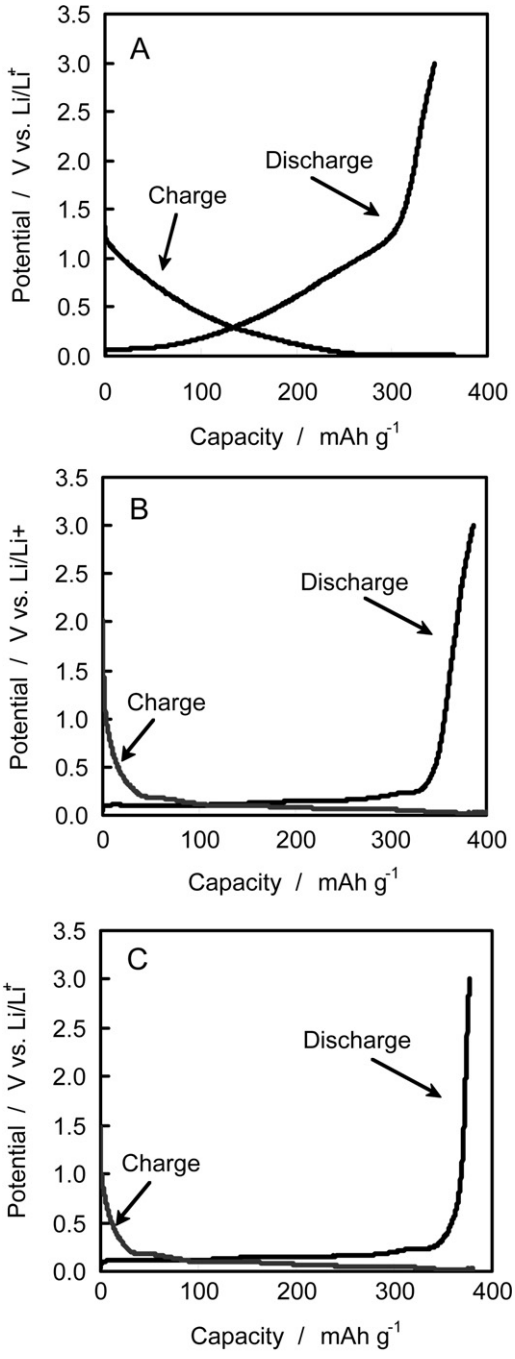

Fig. 2. Charge and discharge curves of HC (A), FG (B) and SG (C) electrodes at C/10 rate in 1.2 M $LiPF_6$/EC3DEC at 25 °C.

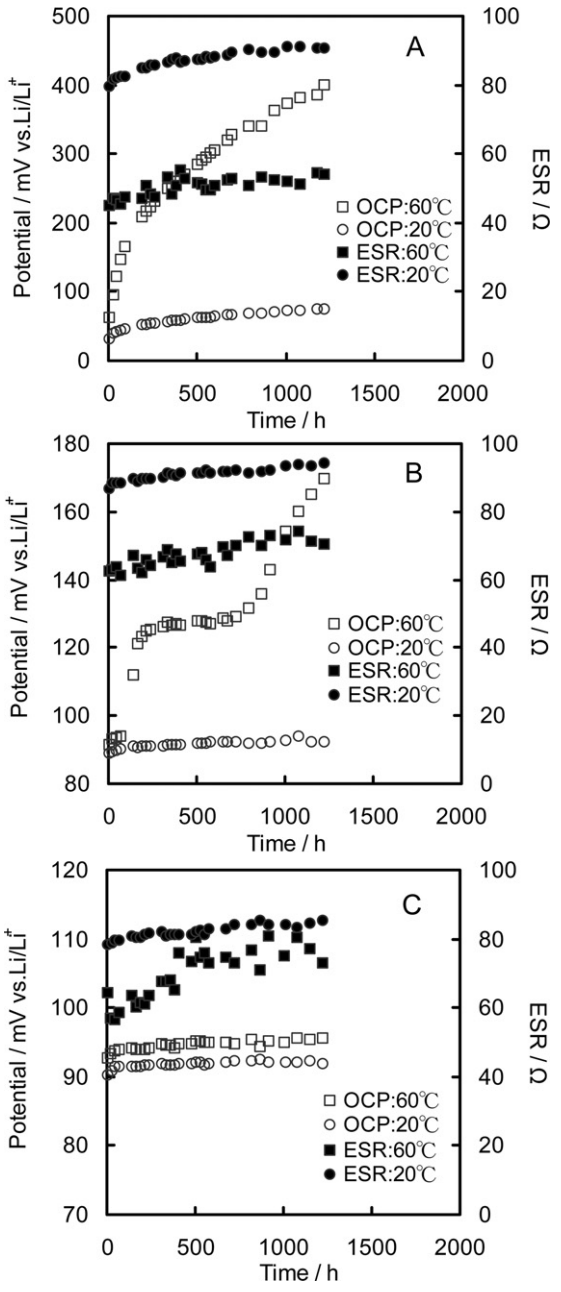

Fig. 3. Variations in OCP (open symbols) and ESR (closed symbols) of HC (A), FG (B) and SG (C) electrodes in 1.2 M $LiPF_6$/EC3DEC at 20 °C (circles) and 60 °C (squares).

3. Results and discussion

Fig. 2 shows typical charge and discharge curves in the second cycle for hard carbon (HC), synthetic flake graphite (FG) and spherical graphite (SG) electrodes in 1.2 M $LiPF_6$/EC3DEC under a current rate of C/10. These potential profiles under the constant current condition showed their own characteristic features [5–7]. The first charge capacity of HC was 459 mAh g^{-1}, while its first discharge capacity was 345 mAh g^{-1}. On the other hand, the charge and discharge capacities of FG were 439 and 386 mAh g^{-1}, respectively, and those of SG were 388 and 377 mAh g^{-1}, respectively. These electrode materials gave stable potential profiles, which were good capacity retention after the second cycle. The irreversible capacity, difference between charge and discharge capacities, of HC was 114 mAh g^{-1}, which was much higher than those of the others. This means that the irreversible capacity of HC would be based not only on the SEI formation but also on the loss of lithium species inside the carbon material. From these data on the irreversible capacity, we determined the quantity of the electricity to charge with ca. 95% state-of-charge (SOC), and then started the self-discharge measurements.

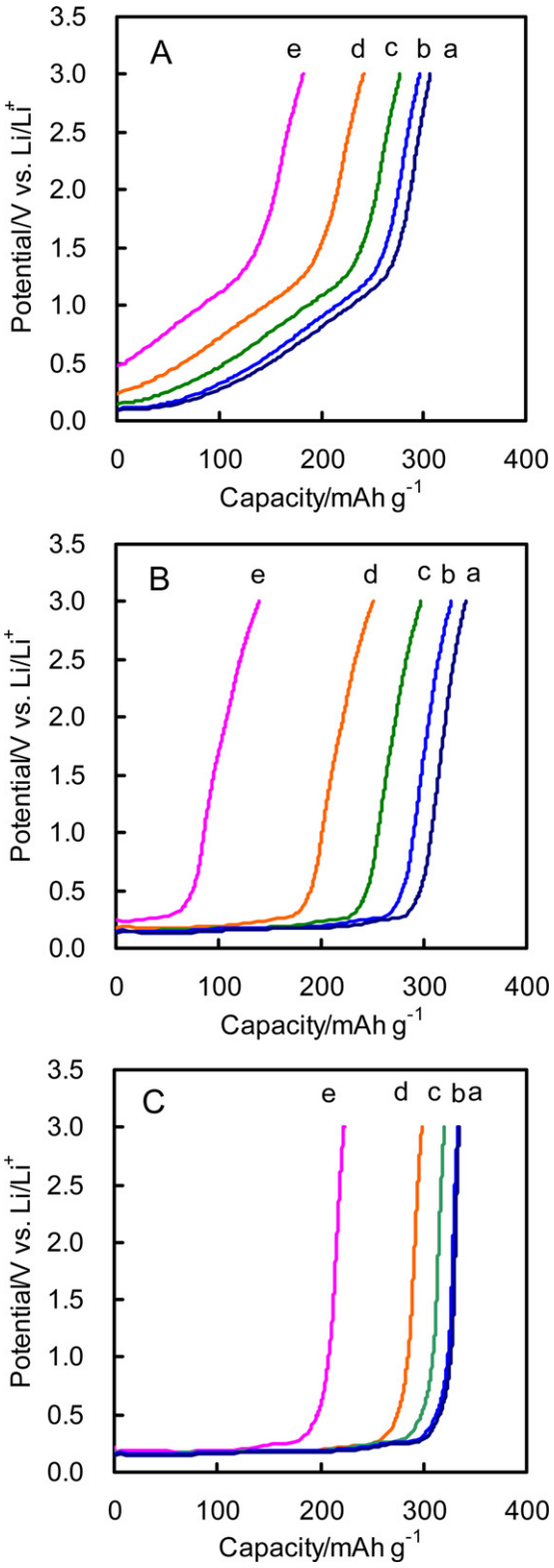

Fig. 4. Variations in discharge curves of HC (A), FG (B) and SG (C) electrodes in 1.2 M $LiPF_6$/EC3DEC after the OCP measurements for 51 days at different storage temperatures of −20 °C (a), 0 °C (b), 20 °C (c), 40 °C (d), and 60 °C (e).

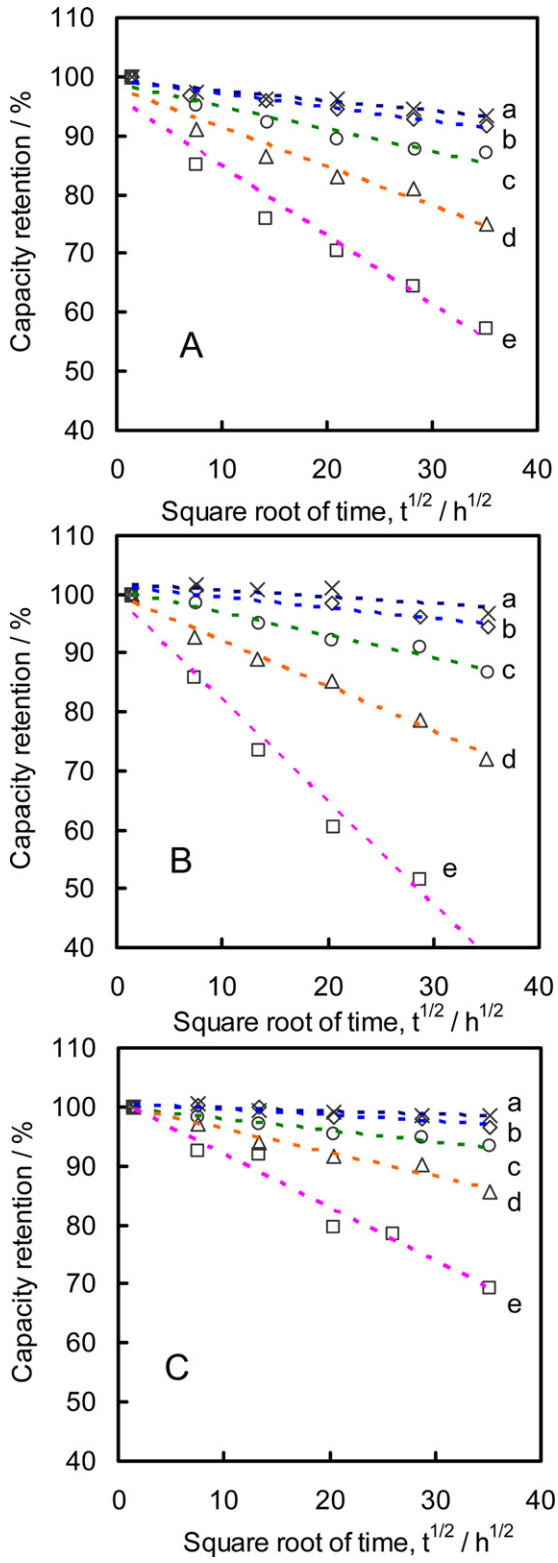

Fig. 5. Variations in the capacity retention with the storage time for HC (A), FG (B) and SG (C) electrodes in 1.2 M $LiPF_6$/EC3DEC at different storage temperatures of −20 °C (a), 0 °C (b), 20 °C (c), 40 °C (d), and 60 °C (e).

In Fig. 3, variations in the open-circuit potential (OCP) and the equivalent series resistance (ESR) after the first charge are plotted against the standing time. The OCP curve of each electrode showed a gradual increase with the time, which gives the same tendency as that of the discharge profile under a constant current polarization,

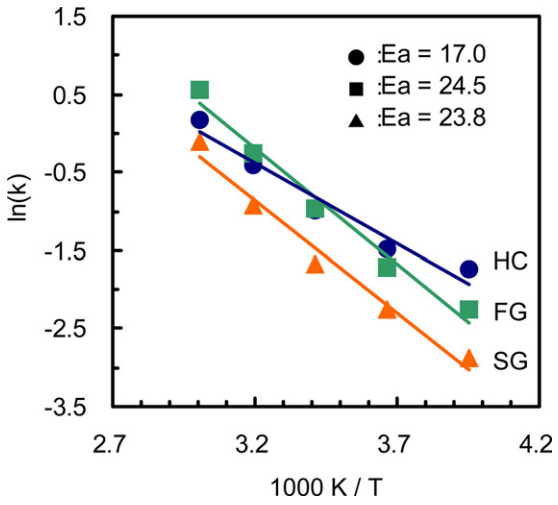

Fig. 6. Arrhenius plots for the rate of capacity loss for HC (●), FG (■) and SG (▲) electrodes in 1.2 M $LiPF_6$/EC3DEC.

as shown in Fig. 1. The OCP profile of charged HC showed gradual changes with the storage time, while both of lithiated graphite-based carbons (FG and SG) respectively gave a potential plateau corresponding to its stage structure of Li-graphite intercalation compound [6,7]. On the other hand, the ESR value of each electrode increased gradually to higher one with the storage time. This suggests that something resistive components form and grow with the passage of the storage time. The rate of the OCP increasing for each electrode was accelerated by elevating the storage temperature.

Fig. 4 shows changes in the discharge capacity after the self-discharge. In every case, the discharge capacity decreased with the storage time. Furthermore, it is clearly shown that the extent of the capacity loss increased with the increase in the storage temperature. From these results, the OCP changes during the storage after the full charging are attributable mainly to the loss of the capacity (Li content in the electrode) during the storage. Heterogeneous reactions of Li species in the electrode and some of the solution components may be possible causes, which form SEI on the electrode surface and/or dissolve in the electrolyte solution [5].

In Fig. 5 the capacity retention is plotted against the square-root of the storage time. Here the discharge capacity is normalized by the capacity after 2 h of self-discharging. The linear relation between the relative capacity and the square-root of the storage time, observed for each electrode, suggests that the self-discharging of the charged carbon electrode is controlled by a diffusion process [8]. The absolute value of the slope of the plot, defined as k, indicates a relative value of the self-discharging rate, which increased with the storage temperature for each electrode. With respect to the kind of carbon material, the self-discharging rate was in the order of SG < HC < FG for every storage temperature. According to the data shown in Table 1, the order of the self-discharging rate at the same temperature corresponds to that of the specific surface area. Thus, these results suggest that both morphology and structure of the carbon material can influence the activity of the Li species in the electrode with the electrolyte components.

Temperature dependences of the k values, so-called Arrhenius plots, are shown in Fig. 6. The correlation factor obtained by the least-square method for the Arrhenius plots was higher than 0.9 in the temperature range between −20 °C and 60 °C, which suggests that the capacity loss is controlled by a consistent process in this temperature range. The activation energy, calculated from the slope of the Arrhenius plot, was about 24 kJ mol^{-1} for the graphite electrodes (FG and SG), and about 17 kJ mol^{-1} for HC. These also indicate that the self-discharging processes at the carbon

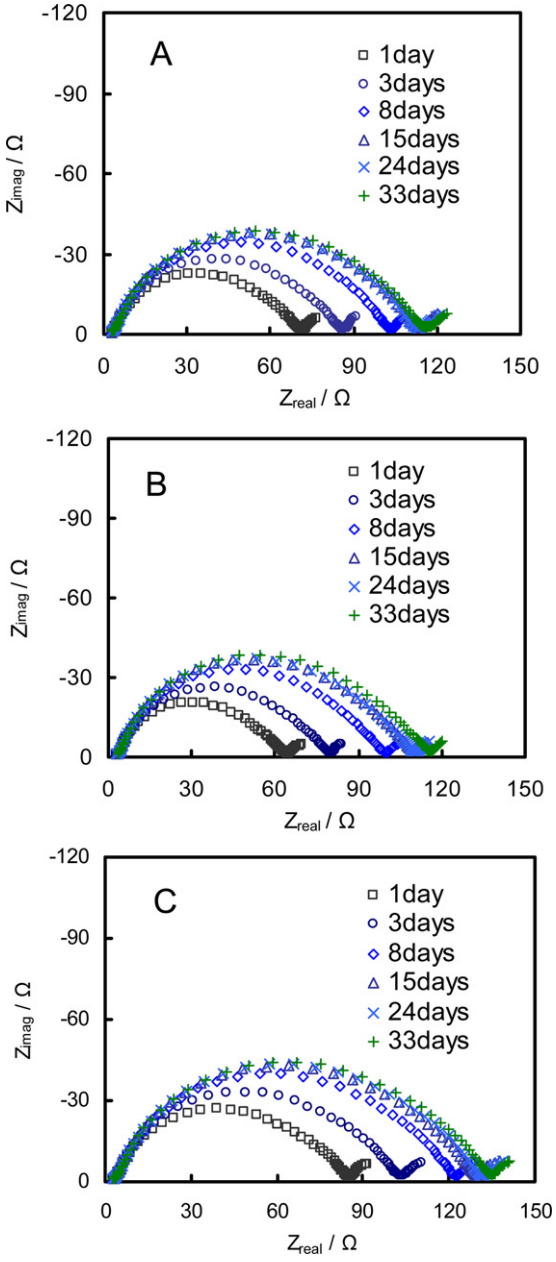

Fig. 7. Variations in the ac impedance with the storage time for HC (A), FG (B) and SG (C) electrodes in 1.2 M $LiPF_6$/EC3DEC at 20 °C.

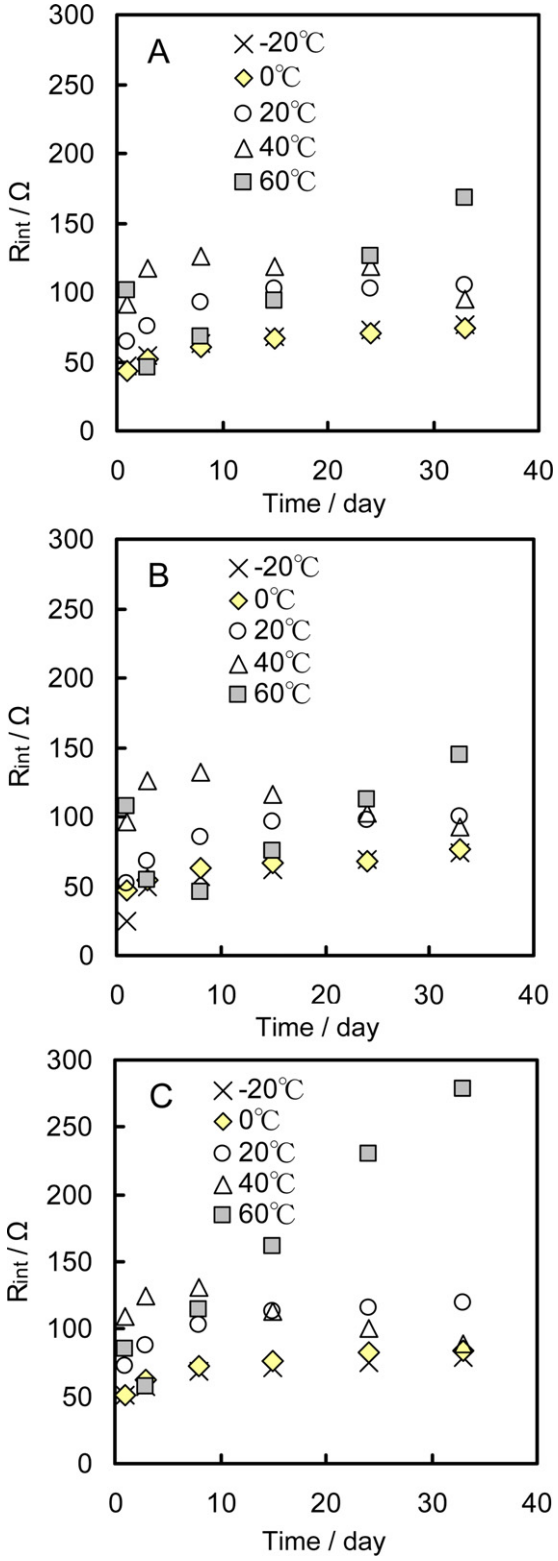

Fig. 8. Variations in the interfacial resistance, R_{int}, with the storage time for HC (A), FG (B) and SG (C) electrodes in 1.2 M $LiPF_6$/EC3DEC at different storage temperatures.

electrodes are controlled by mass-transfer steps. If the processes include the formation of SEI at the electrode surface, diffusion of Li species in the solid phase will be rate-controlling. These results are consistent with the previously reported one for PAS electrode in organic electrolyte solutions, where the SEI forming additives worked effectively to prevent further progress of self-discharging [5].

The ac impedance responses for lithiated carbon electrodes at 20 °C are shown in Fig. 7, as a function of the storage time after the first charge. Every Nyquist plot of the impedance consists of a semicircle in the higher frequency region and a short arc in the lower frequency region. The size of the semicircle generally increased with the storage time in its early stage. As the resistance component in this frequency region is attributable to the interface process, we defined it as "interface resistance", R_{int}. It tends to increase with increasing SOC, since it conjugates partly with the charge-transfer resistance, R_{ct}. However, the main reason of the increase in R_{int} with the storage time should be based on the growth of SEI on the electrode surface. On the other hand, the bulk resistance R_{bulk}, which is determined from the intersection of the semicircle at higher frequency region, does not change significantly during the storage. Thus, we can exclude any possible influences of the electrolyte deterioration itself on the present impedance measurements.

The variations in the ac impedance response with storage time were monitored at different temperatures. Fig. 8 compares the variations in R_{int} with the storage time measured for different carbon materials at different temperatures. For every electrode, variations in R_{int} with time were rather small at lower temperature (<0 °C). On the other hand, for the storage at 60 °C, the R_{int} value monotonously increased with time, after the small decrease in the early stage of the storage (<4 days). The storage at moderate temperatures (20 °C and 40 °C) showed characteristic profiles in R_{int} variations that have maxima at 8–24 days. Although the exact reasons for these complicated features of the variations in the interfacial resistance are unclear at the present, a following scheme is possible to explain the experimental results. The main causes of varying R_{int} would be changes in the thickness of the surface film, SEI, and in the SOC of the electrode with time. At low temperature, as the self-discharging rate corresponding to the film growth rate is relatively low, the interfacial resistance increases slowly and monotonously with the storage time. During the storage at higher temperature, e.g. 60 °C, a higher rate of the film formation causes a significant increase in the interface resistance along with the storage time, after initial drop within few hours. In the moderate temperature range (20–40 °C), the growth of the SEI layer increases the interfacial resistance, but lowering SOC caused by self-discharging decreases the charge-transfer resistance, whose balance may come out on the resistance variation with a maximum value at certain period of the storage. Thus, the time (day) giving maximum resistance depended on the storage temperature and the carbon material, both of which influence the rates of film formation and capacity loss.

With respect to the sort of the carbon material, almost the same profiles were observed for the changes in R_{int} with the storage time in the temperature range below 40 °C. This is probably because of the same process occurring on each carbon material. For example, the FG sample has higher specific surface area and showed higher self-discharging rate than the other carbon samples, but the rate of SEI formation at FG per real surface area will be almost the same as the others. On the other hand, for the storage at higher temperature of 60 °C, the increasing rate of R_{int} for SG was apparently higher than those for HC and FG. This suggests that the film formation process on the SG surface is somewhat different from that on HC and FG at higher temperature. In general, the self-discharge process accompanying the decrease of the discharge capacity has some relationship to growth of the SEI layer on each carbon electrode, although there still remain details of its mechanism unclear. The surface process at the carbon electrodes during the self-discharging is now under investigation, whose results will be published in near future.

4. Conclusion

Self-discharging characteristics of different carbon electrodes have been investigated by monitoring the open circuit potential (OCP) accompanied by the capacity loss and measuring the impedance change during the storage at different temperatures. The results are summarized as follows.

(1) The time-profile of OCP reflecting the state-of charge (SOC) depended on both the carbon material and the storage temperature. Higher specific surface area and higher storage temperature lead to higher self-discharging rate.
(2) The activation energy, estimated from the temperature dependence of the self-discharging rate, at hard carbon electrode was slightly lower than those at graphite electrodes. It suggests that the self-discharging reaction at each electrode is controlled by a diffusion process.
(3) Changes in the interfacial resistance determined from ac impedance revealed that the rate of SEI formation at lower temperature does not depend on the carbon material. However, at higher temperature, the SEI formation rate at spherical graphite was much higher than those at the other carbon materials.

References

[1] B. Scrosati, J. Garche, J. Power Sources 195 (2010) 2419.
[2] J. Vetter, P. Novák, M.R. Wagner, C. Veit, K.-C. Möller, J.O. Besenhard, M. Winter, M. Wohlfahrt-Mehrens, C. Vogler, A. Hammouche, J. Power Sources 147 (2005) 269.
[3] R. Yazami, Y.F. Reynier, Electrochim. Acta 47 (2002) 1217.
[4] M. Holzapfel, Alloin, R. Yazami, Electrochim. Acta 49 (2004) 581.
[5] K. Ohue, T. Utsunomiya, O. Hatozaki, N. Yoshimoto, M. Egashira, M. Morita, J. Power Sources 196 (2011) 3604.
[6] R. Yazami, M. Deschamps, S. Genies, J.C. Frison, J. Power Sources 68 (1997) 110.
[7] M. Noel, V. Suryanarayanan, J. Power Sources 111 (2002) 193.
[8] A.J. Bard, L.R. Faulkner, Electrochemical Methods; Fundamentals and Applications, 2nd ed., John Willey & Sons, New York, 2001 (Chapter 4).